RESEARCH ARTICLE                                                        OPEN ACCESS

# Modification of Recycled Al-332 Alloy Using Manganese Dioxide

## *Durowoju M.O. and Babatunde I.A.
Department of Mechanical Engineering, Ladoke Akintola University of Technology, Ogbomosho

**ABTRACT**
Aluminum and its alloys are commercially available materials for both domestic (cooking utensils, beverages can) and industrial applications (automobile and aircraft structural parts). This study presented the effect of the use of manganese dioxide ($MnO_2$), obtained from discarded dry cell batteries on the features and formation of pores in recycled pistons (Al-332 alloy).
3kg of recycled Al-332 alloy was obtained in form of ingot. 150 g of the ingot was re-melted and the molten alloy was treated with 2 to 12g of $MnO_2$. The molten alloy was stirred gently for 1 minute, sand cast and normalized. Parts of the cast samples were used for microstructural analysis, tensile strength and hardness test following standard test procedures in accordance with ASTM E8M-91 standards (1992). The distribution of pores present in the cast alloys were studied using fractal analysis and spatial point pattern method (SPP). The hardness, tensile strength, average fractal dimensions and sphericities were related to the amount of $MnO_2$.
The micrographs revealed an absolute reduction in pores at 8gram addition of $MnO_2$. Maximum hardness and tensile values of 50.8BHN and 65.01MN/m$^2$ were obtained at 8 g addition of $MnO_2$, above which there is decrease in properties of the material. The weighted average fractal dimension and sphericity for as-cast and sample treated with 8 g of $MnO_2$ are 1.3276 and 0.3357; 1.0050 and 0.9918 respectively. Spatial point pattern revealed that the pores in the samples are randomly distributed.
The study has established that manganese dioxide is a good modify for recycled Al-332 alloy. It improved the mechanical properties of the alloy and reduce the pores in the cast sample to the barest minimum.
*Key words:* Recycled Al-332 Alloy, $MnO_2$, Fractal Analysis, Spatial Point Pattern

## I.    Introduction

Aluminum recycling has significant environmental and economic benefits. With energy and cost savings in mind, many producers now have targets of increasing their usage of recycled materials. It has been well demonstrated that the presence of unwanted elements, dissolved gases and non-metallic inclusions greatly enhances the porosity formation in aluminum alloys making it act as stress-raisers and cause premature failure of components (Miller *et al*., 2002; Hussein *et al*., 2013). Over the years, a number of test methods have been developed for inclusion detection in liquid aluminum (Paraskevas *et al*., 2013), but the general experience in the casting industry has been that these techniques were usually slow, inappropriately complicated and/or expensive for use on the foundry floor.

Recently, the production of premium quality castings for the structurally safe components for automotive applications requires that porosity and inclusions be minimized or eliminated to negate their harmful influence on the mechanical properties. Kim *et al*., (2006) revealed that in order to achieve a competitive advantage in the automotive industry it has become necessary to use Al-alloy scrap to keep the cost-down. However, the Al-alloy recycling process requires a wide range of control techniques to meet tight criteria on quality. To this end, many researchers established the treatment of molten metal with modifiers or grain refinements (Kósa *et. al*., 2012; Stunová, 2012; Farahany, 2011) to reduce or eliminate pores in Al-alloy and also improve its mechanical properties. This aim of this work is to study the effect of the use of $MnO_2$ on the features and formation of pores in recycled Al-332 alloy.

## II.    Experimental Procedure
### 2.1 Secondary Al-332 Alloy

The molten metal used in this study was obtained from scrap aluminum alloy pistons Al-332. These were melted in an open furnace and the melt was cast into ingots form 150g. The chemical composition of the alloy and black powder (obtained from discarded dry cell battery) Figure 1, were carried out via Minipal 4 Spectrometry, Table 1 and 2. The analysis revealed that the piston has major alloying elements of Al-13.68Si-2.4Mg alloy. The ingots of 150g each were then re-melted and treated with 2 to 12 grams of manganese dioxide ($MnO_2$) heated to a temperature of 700° C ± 5° C, with holding time of 2-3 minute. The melt was gently stirred for 1 minute to ensure homogeneity in the entire mixture and then cast into a sand mould. This process was repeated for all the samples. After solidification the moulds were broken and the samples were machined according to ASTM-E8 standards for the tensile testing Figure 2. 20mm cylindrical rods were cut from each sample,

grounded, polished and etched prior to microstructural analysis (optical metallurgical microscope with 10X10 magnifications).

**Table 1:** Chemical Composition of Al-332 alloy (wt%)

| Materials Elements | Si | Cu | Mn | Mg | Fe | Zn | Ni | Pb | Cr | Ti | Be | Bi |
|---|---|---|---|---|---|---|---|---|---|---|---|---|
| % Composition | 13.68 | 1.08 | 0.197 | >2.40 | 0.35 | 0.249 | 0.62 | 0.035 | 0.016 | 0.032 | <0.0001 | <0.001 |

| Ca | Sn | Co | Na | P | Sr | V | Zr | Cd | Al |
|---|---|---|---|---|---|---|---|---|---|
| 0.0004 | 0.01 | <0.001 | <0.0001 | 0.001 | 0.0001 | 0.014 | 0.0026 | 0.0012 | balance |

**Table 2:** Composition of the Discarded (or Used) Battery (wt%)

| Elemental Constituent | MnO | ZnCl | NHCl$_3$ | FeO | PbO | Gel | Others (unidentified) |
|---|---|---|---|---|---|---|---|
| % Composition | 23.25 | 3.16 | 2.13 | 5.65 | 0.105 | 0.05 | ----- |

Damp black powder
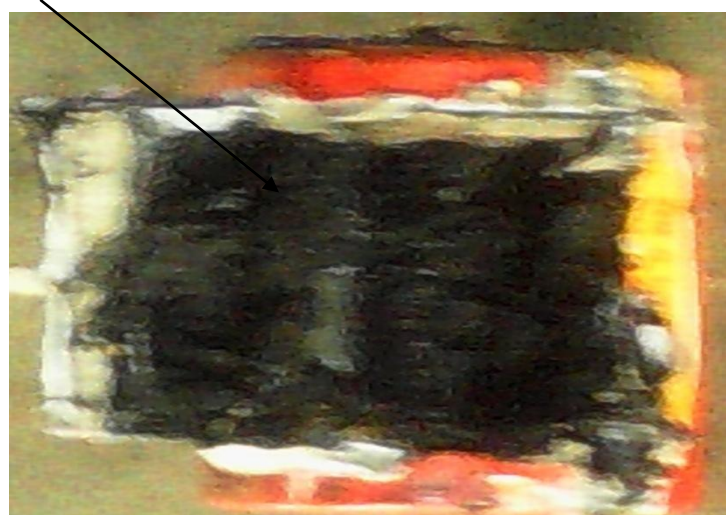


**Figure 1:** Schematic diagram of a typical dry cell battery showing the blank constituent
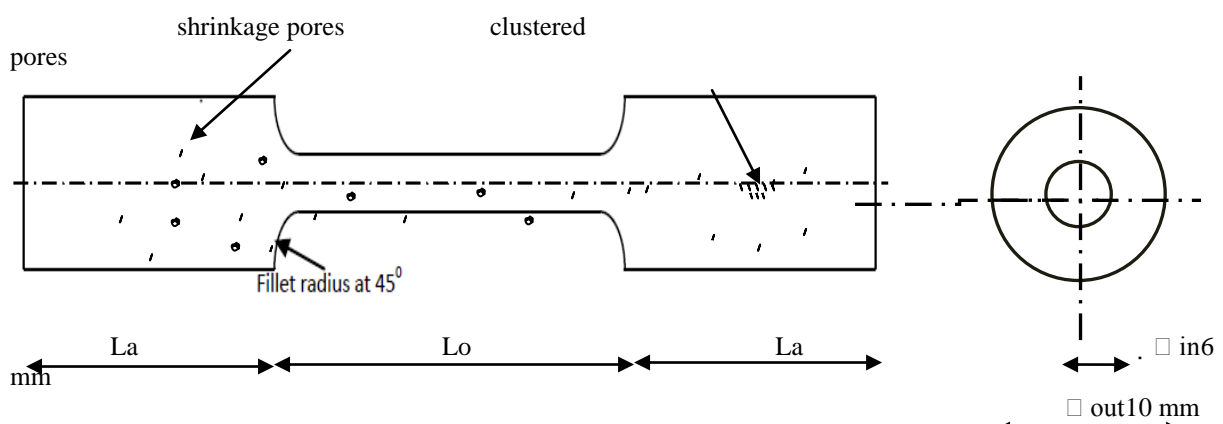


**Figure 2:** Test specimen from as-cast. ⬜ out= Diameter of gripping heads; ∅$_{in}$ = Diameter of the gauge length; La = Minimum gripping length; Lo = gauge length.

### 2.2 Characterization of Porosity Using Fractal Approach

Porosity is a very common defect in aluminum castings. Figure 5 shows a typical view of microstructure of unmodified Al-332 alloy with shrinkage and gaseous pore. It is known that the quantity and the appearance of the porosity are very crucial to the mechanical properties of the casting, especially an application where cyclic loading will be involved (Lu and Hellawell, 1995; Monroe, 2005). Porosity sources include entrapped air during filling, shrinkage that occurs during the final solidification, blowholes from unvented cores, reactions at the mold wall, dissolved gases from melting and dross or slag containing gas porosity (Compbell, 2003).

In this study, fractal analysis of pores in Al-332 alloy was examined. Fractal geometry was firstly developed by Mandelbrot (1982). Its principle is universal in any measurement and has been previously used by many researchers to numerically describe complex microstructures including graphite flakes and nodules (Lu and Hellawell, 1994). In this work, an interactive Matlab program was developed to obtain the numerical values of the fractal dimension $D$ and the sphericity $\beta$. To develop the program the box counting method was used with a counter incorporated into the program and the small boxes or pixels occupied by the pores outlines are counted. In all, four pixels (2x2 pixels, 4x4 pixels, 8x8 pixels and 16x16pixels) and four grid sizes (200x200, 100x100, 50x50 and 25x25) were selected. The selections were made for better resolution and to obtain accurate values.

The distribution of the pores in recycled AlSi2.4Mg alloy was done using Spatial Point Pattern Method (SPP) Figure 3. The pore distribution maps (Figure 4) was also constructed to identify the shapes of the pores and their dispersion from regular shapes.

The Mathematical basis for measuring chaotic objects with the power law modified is adopted in this work. The basic equation is as follows:

$$P = P_E \, \delta^{D-1} \text{ (for } 1 < D < 2 \text{ and}$$

$$\delta_m < \delta < \delta_M) \qquad \dots\dots\dots\dots\dots(1.1)$$

Where $P_E$ is the measured perimeter, $P$ is the true perimeter, $\delta$ is the yardstick, $\delta_m$ and $\delta_M$ are the lower and upper limits respectively for any shape and $D$ is

defined as the fractal dimension ($1 < D < 2$). From this relationship, it can be deduced that the true perimeter is actually a function of yardstick for measurement. The fractal dimension, $D$, therefore describes the complexity of the contour of an object which is practically called the roughness Figure 3, (Durowoju et al., 2013). When $\delta < \delta_m$, the measurement is not sensitive to the yardstick chosen, giving a smaller value of the slope. However, when $\delta > \delta_M$, the size of the yardstick exceeds that of the individual feature being measured so that the measurement loses meaning because the object falls below the resolution limit of the yardstick used for measurement (Durowoju, 2013; Durowoju et al., 2013).

Sphericity, $\beta$, is another dimensionless number used together with roughness, $D$, to describe the shape of the pores formed. That is;

$$\beta = 4\pi A_T / P^2 \qquad \text{(for } 0 <$$

$$\beta < 1 \text{ and } 1 < D < 2) \qquad \dots\dots\dots\dots\dots(1.2)$$

Substituting equation (2.10) in equation (2.11) gives

$$\beta = \left(4\pi A_T / P_E^2\right) \delta^{2(1-D)} \qquad \text{(for } 0 <$$

$$\beta < 1 \text{ and } 1 < D < 2) \qquad \dots\dots\dots\dots\dots(1.3)$$

Where $A_T$ is the total pore area, when $\beta = 1$ and $D = 1$, a perfect circular shape is formed by the pores in the microstructure. However, as $\beta$ decreases, the shapes become more elongated showing a departure from perfect sphere. The locations of $1 < D < 2$ represent less regular shapes.

To calculate the perimeter $P$ of the pores, the Slit Island Method (SIM) introduced by Mandelbrot (1983) was used. It is expressed as:

$$\log_e P = 0.5 \, D \, \log_e A_T$$

$$\log_e P = \log_e A_T^{D/2} \qquad \dots\dots\dots\dots(1.4)$$

$$P = e^{0.5 \, D \, \log_e A_T}$$
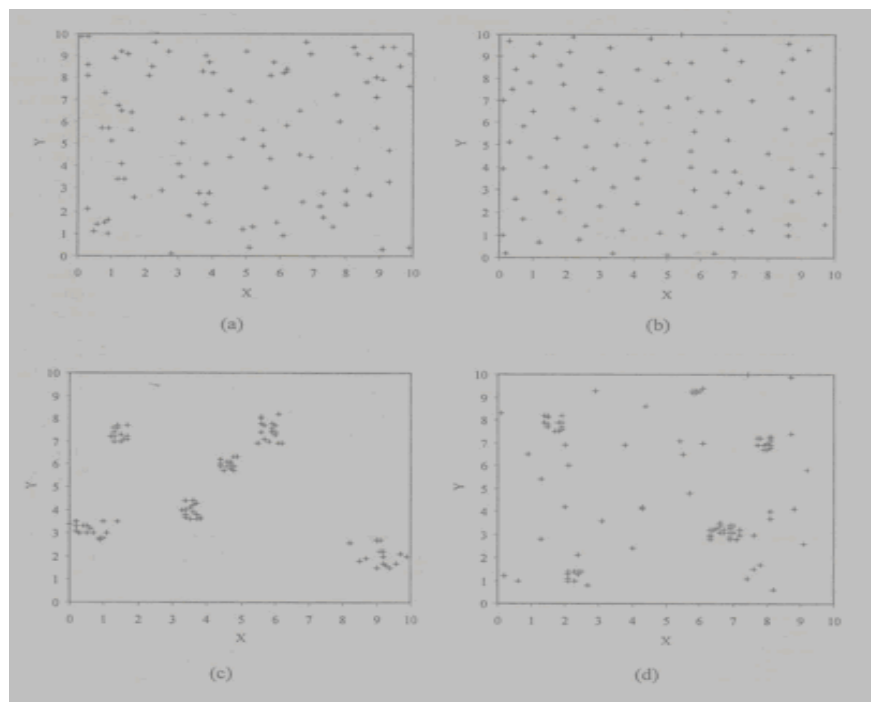
**Figure 3:** The four common types of spatial point patterns
(a) random, (b) regular, (c) clustered, (d) clustered superimposed on random background.
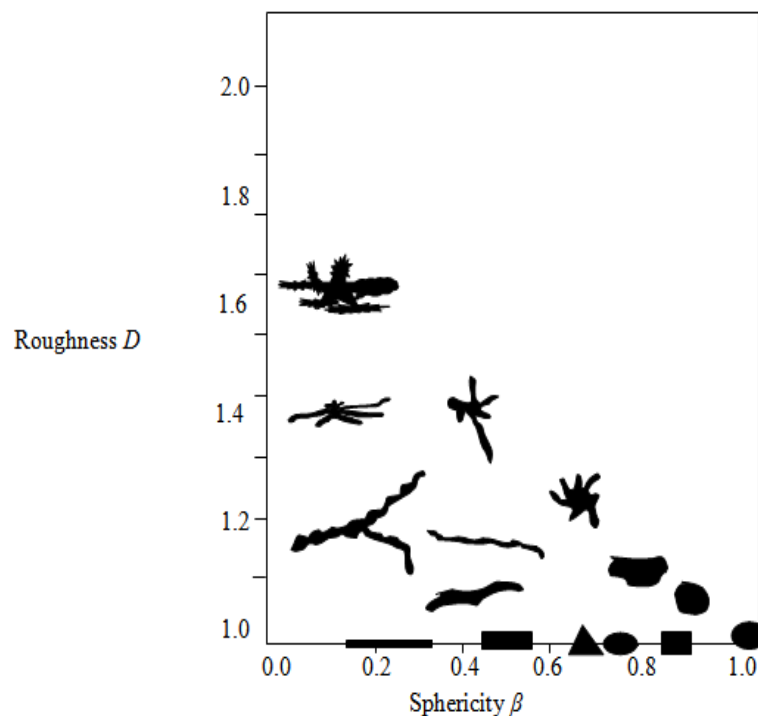


**Figure 4:** Illustration of development of irregular shapes based upon Euclidean circle or rectangle.
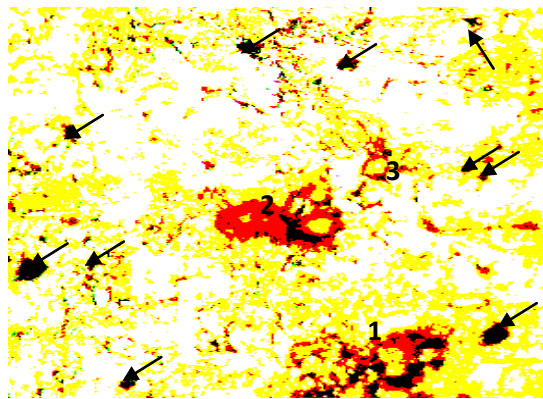
**Figure 5:** A typical view of unmodified Al-332 alloy: showing both the gas pores (arrow) and shrinkage pores (numbers)
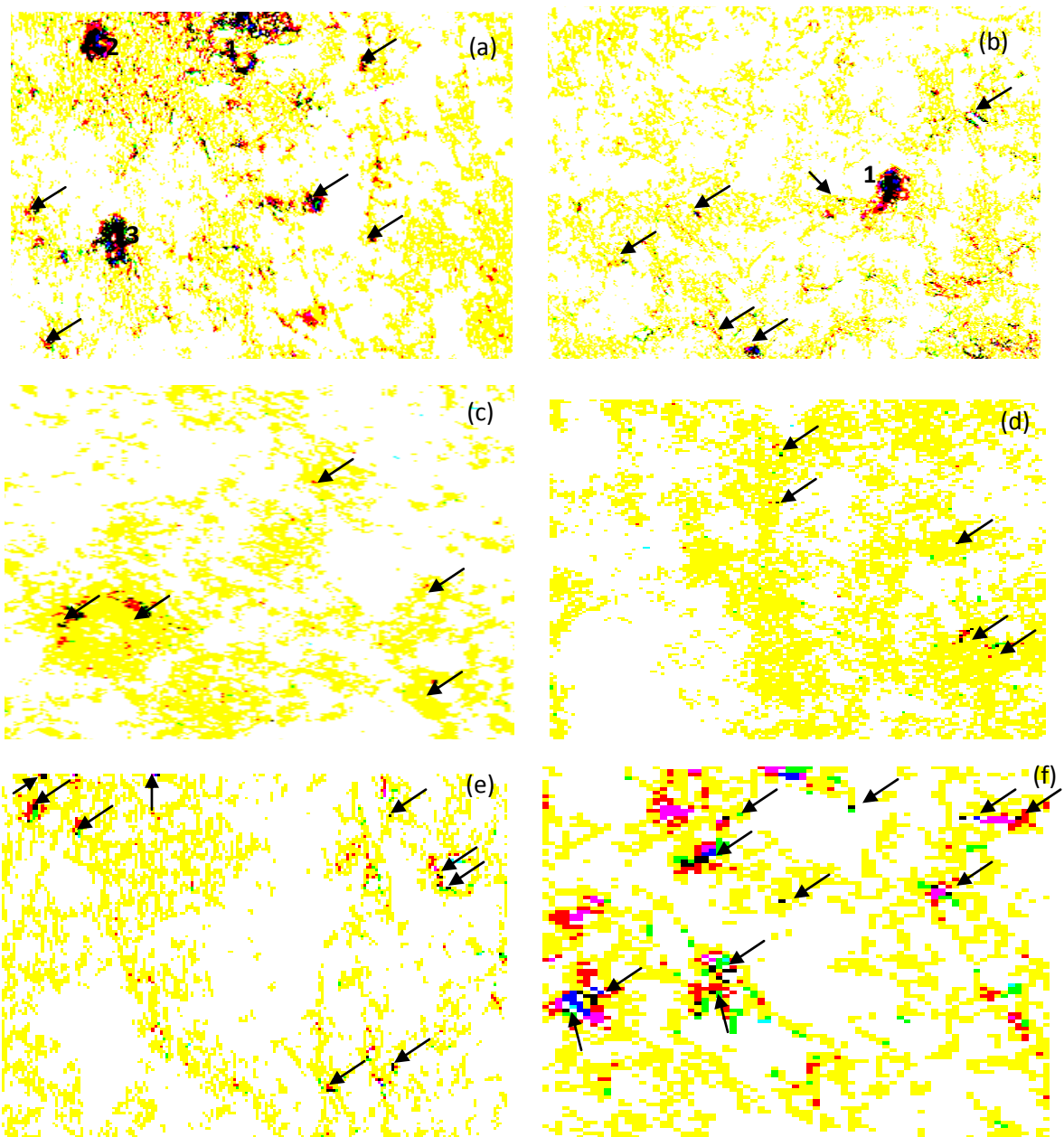


**Figure 6:** Micrographs of Al-332 alloy modified with different amount of $MnO_2$
(a) 2g; (b) 4g; (c) 6g; (d) 8g; (e) 10g; (f) 12g.

## III. Result and Discussion

The hardness values of the samples increases with increasing $MnO_2$ up to 8gram addition and partially decreases from 10g to 12g. This shows that $MnO_2$-modified Al-13.68Si-2.4Mg alloy has an optimal hardness of 56.2 BHN at 8g. Equally, the tensile strength (TS) increases with increase in $MnO_2$ (Figure 7). Maximum tensile strength of 65.01 $MN/m^2$ was obtained at 8g addition of $MnO_2$. After this point, there is a significance decrease in the tensile strength of the material. The reasons for this may be attributed to the fact that the size and shape of the pores within the microstructure tends to be more irregular and their distributions become more clustered allowing the pores to easily link one another causing reduction in tensile strength of the material. Apart from this, large amount of $MnO_2$ seems to add unwanted impurity to the molten metal, thereby reducing the mechanical properties of the material.

Figures 5 and 6 show the micrographs of the unmodified and samples treated with $MnO_2$. Pores selected from unmodified micrograph were fed into the computer program to evaluate their fractal dimensions and sphericities. This was done for the remaining microstructures to evaluate the parameters of the pores. Above all, the fractal dimensions and sphericities of each pore are then analyzed.

From Figure 5 and 6, it is obvious that there are more shrinkage pores in the unmodified alloy compared with modified Al-332 which has more gaseous pores that are relatively small and regular in shape.

A series of quantitative metallographic analyses carried out on the unmodified and modified samples of recycled Al-332 alloy indicate that the shape and size of the pores are affected by the amount of manganese dioxide ($MnO_2$) added to the molten metal. It was found that the fractal dimension *D,* and sphericity *β*, of the pores changed from irregular to rounded or more regular shapes as the amount of $MnO_2$ increases. It was also observed that the inter-spacing between the pores increases. This effect was more pronounced in the samples modified with 6g and 8g of $MnO_2$. The present results revealed that $MnO_2$ reduces the pores in recycled Al-332 significantly.

Figures 8-14 presented the pore distribution maps of each of the microstructure as obtained from the fractal analysis. Each data point represents an individual pore and the big-sized data point represents the weighted average of the pores' sphericities and fractal dimensions respectively. Figure 8 shows the pore distribution map for unmodified sample. It was observed that the pores are generally clustered having a weighted average sphericity and fractal dimensions (roughness) of 0.6710 and 1.0749. Figure 9 shows the pore distribution map for sample modified with 2g addition of $MnO_2$. It was observed that the pores are generally clustered on random background having a weighted average sphericity and fractal dimension of 0.6574 and 1.1004.

Figure 11 and 12 show the pore distribution maps for sample modified with 6g and 8g addition of $MnO_2$. It is evidence from the micrograph that the pores are randomly distributed as the shape of the pores had attained regular domain. Weighted average values of sphericity and fractal dimension of 0.9231 and 1.0819; 0.9826 and 1.0282 were obtained.

Figure 13 and 14 revealed that the shape of the pores tends to be clustered on random background. Compared with the unmodified sample, there is significant improvement in the sphericities of modified samples.
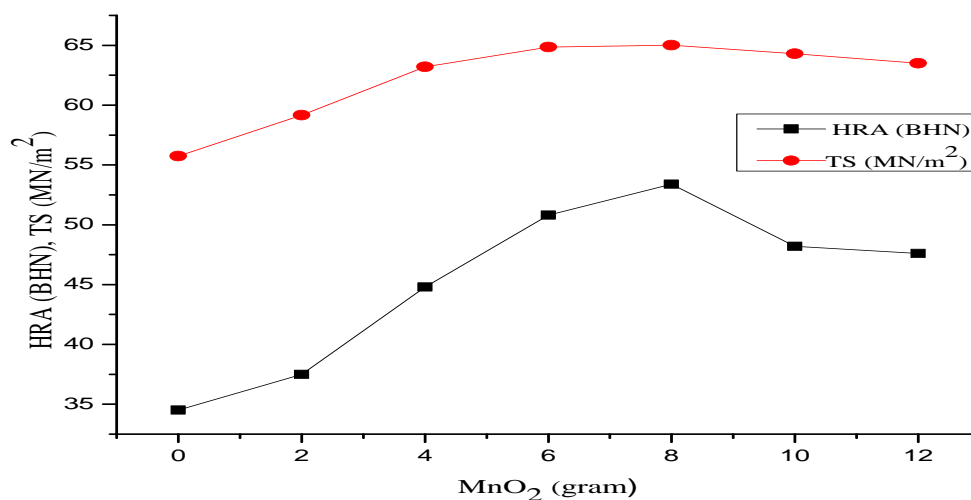


**Figure 7:** Variation of the Hardness (HRA) and Tensile Strength (TS) against $MnO_2$
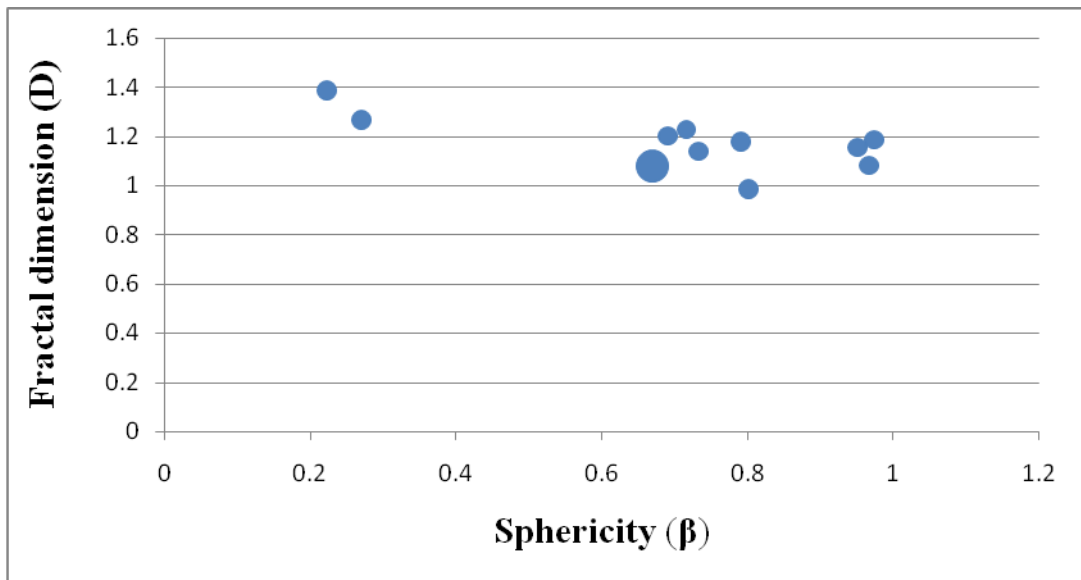
**Figure 8:** Pore Distribution Map for Unmodified Al-332 Alloy

Huang and Lu, (2002) observed that shrinkage pores are usually larger in sizes and of more irregular than gaseous pores. This study revealed that there exists a critical value of the sphericity, by which the two types of pores can be separated and this value, from our numerical measurements, seems to be $\beta < 0.38$ which is in agreement with the study conducted by Huang and Lu, (2002). Thus, the pores with $\beta <$ 0.38 are normally shrinkage pores and the pores with $\beta > 0.38$ are normally gaseous pores. With this criterion, it was very easy to calculate the percentage of such different porosities. From this analysis, we found out that the unmodified sample70% of pores in a sample are gaseous type and the rest are the shrinkage pores.
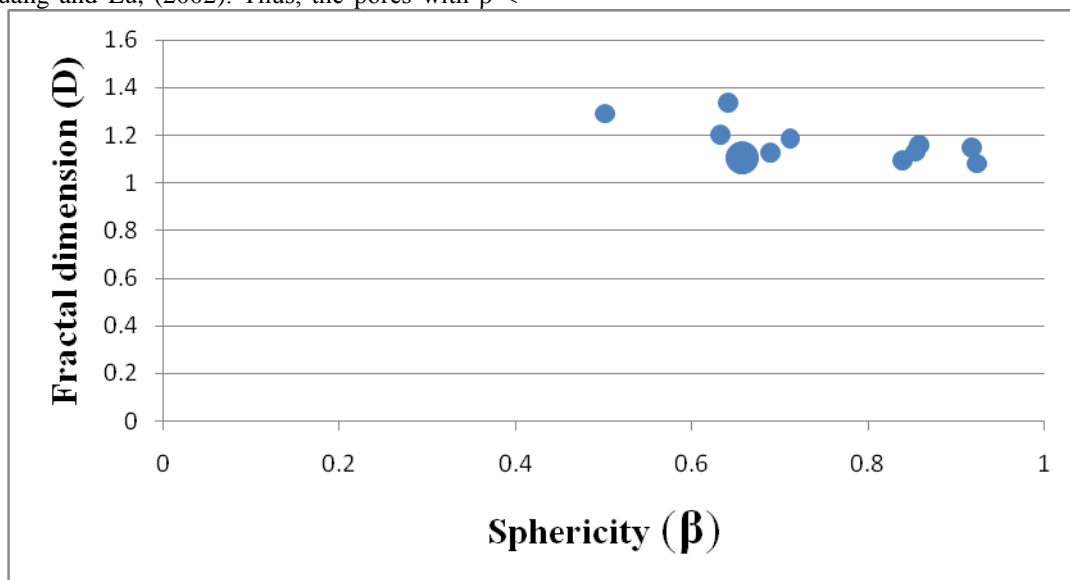


**Figure 9:** Pore Distribution Map for Al-332 Alloy modified with 2g of $MnO_2$
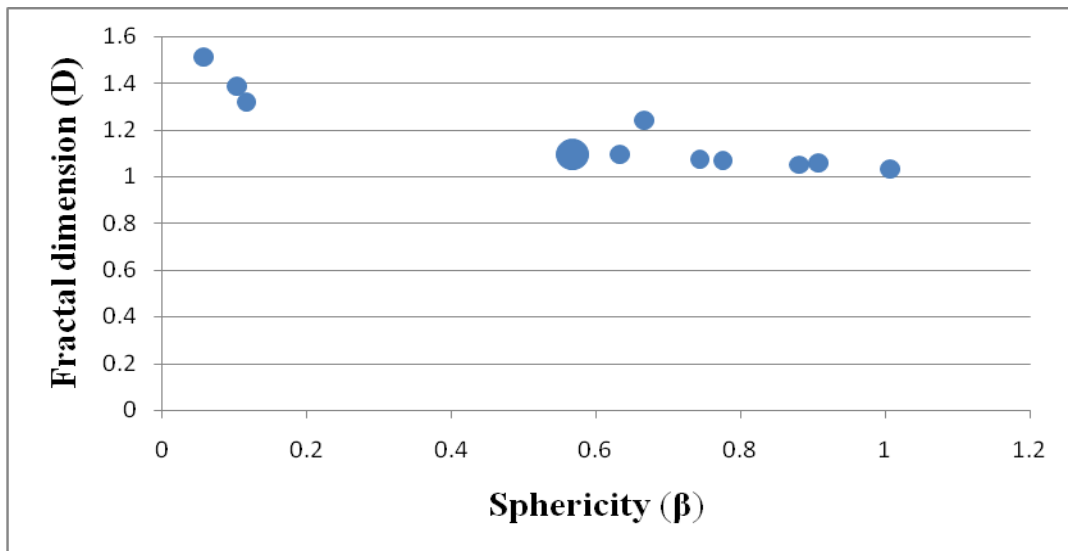
**Figure 10:** Pore Distribution Map for Al-332 Alloy modified with 4g of $MnO_2$
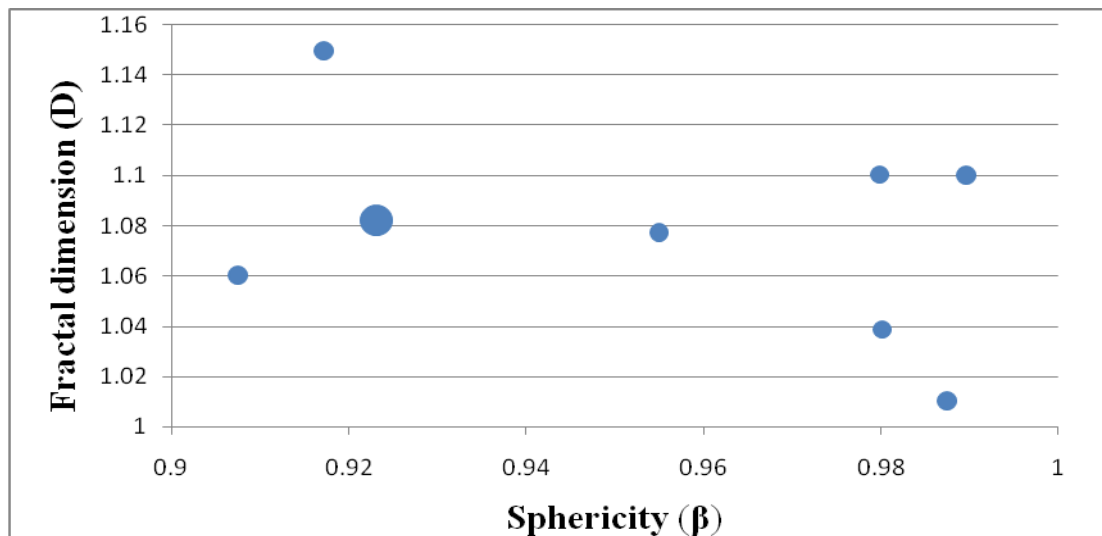
**Figure 11:** Pore Distribution Map for Al-332 Alloy modified with 6g of $MnO_2$
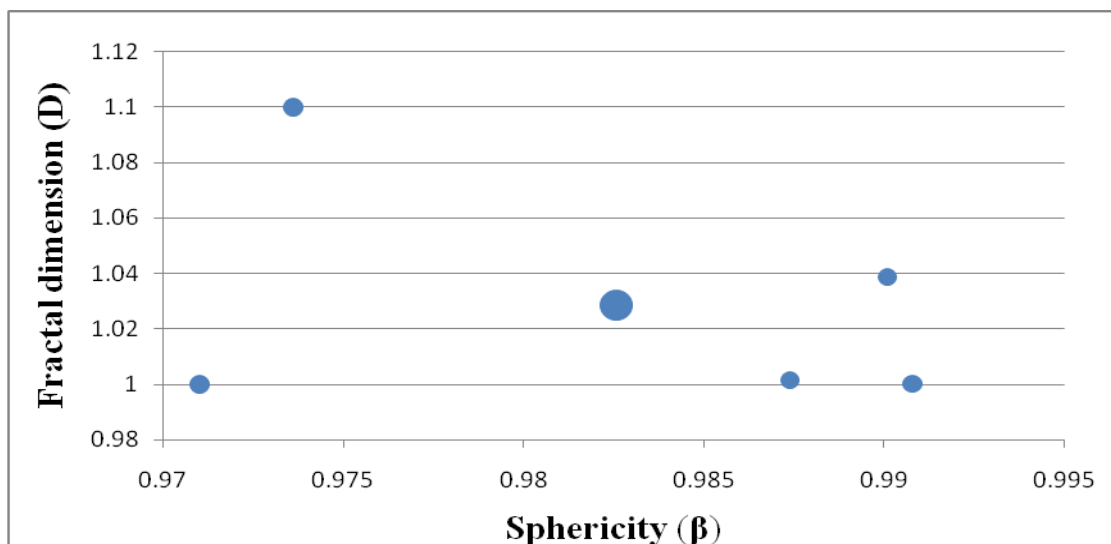
**Figure 12:** Pore Distribution Map for Al-332 Alloy modified with 8g of $MnO_2$
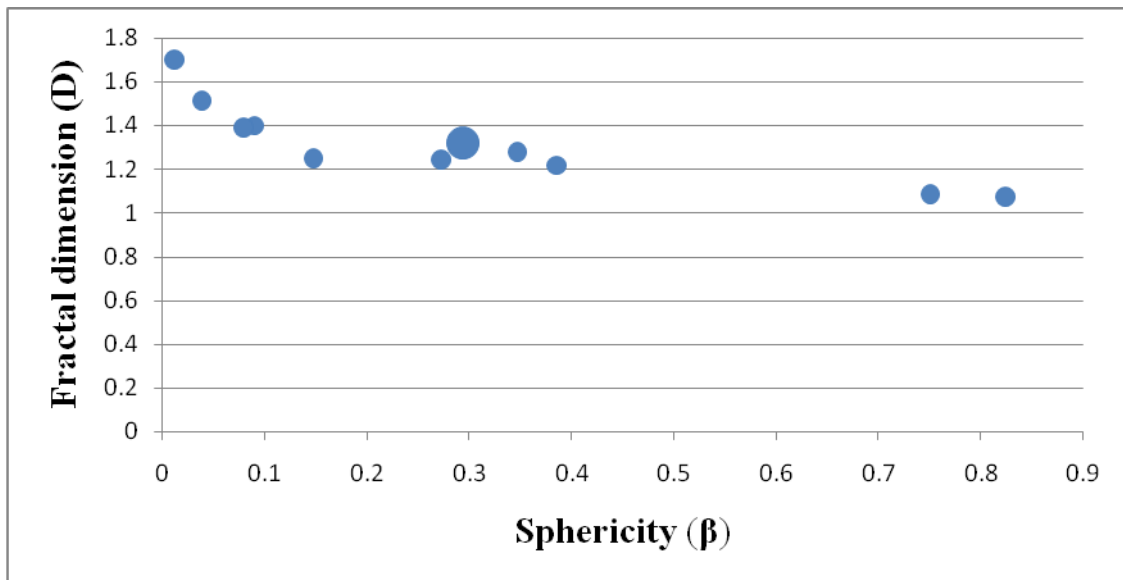
**Figure 13:** Pore Distribution Map for Al-332 Alloy modified with 10g of $MnO_2$
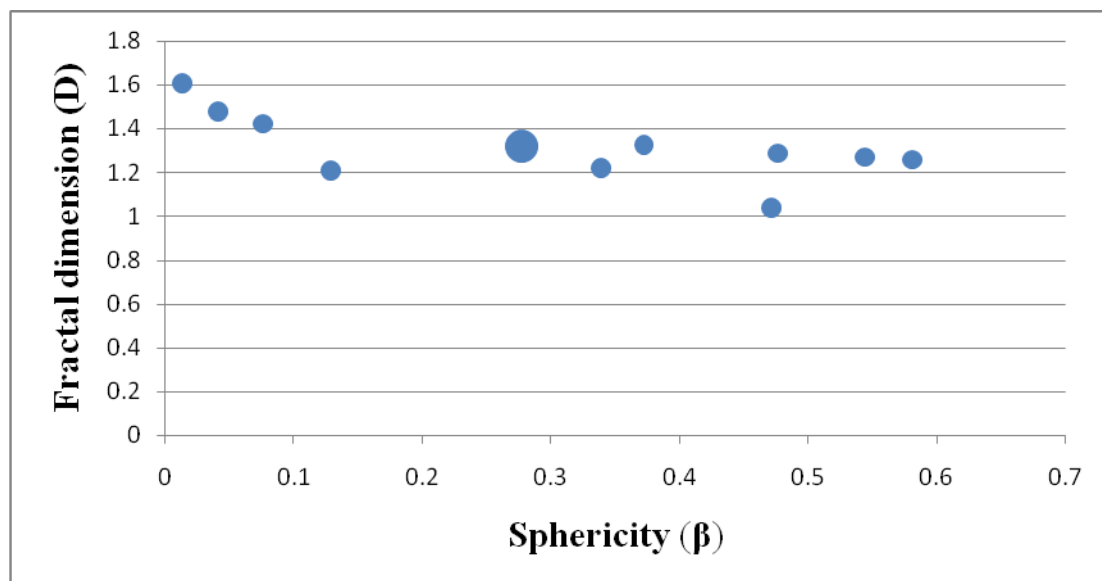
**Figure 14:** Pore Distribution Map for Al-332 Alloy modified with 12g of $MnO_2$

## IV. Conclusion

1. Fractal analysis can be applied to the porosity measurement to describe the shapes and sizes of the pores in recycled aluminum alloys using two dimensionless parameters, Fractal dimension, *D* and Sphericity, *β*. This method may complement with the conventional quantitative examination for porosity.

2. It was observed that the shrinkage pores are more pronounced in untreated alloy and alloy treated with small amount of $MnO_2$. At higher amount of MnO2, shrinkage pores were totally eliminated and gaseous pores were also reduces in both shapes and sizes.

3. It was also found that the smaller the percentage of pores, the higher the tensile strengths of the materials. This is evidence form both the microstructures and the mechanical properties.

## Reference

[1] Compbell, J. (2003), "*The new metallurgy of casting metals*", 2nd edition, New York.

[2] Durowoju, M.O., (2013); "*Numerical Characterization of the Pores and the Determination of the Point Of Crack Initiation in Some Cast Aluminum Alloys*", International Journal of Modern Engineering Research, Vol.3, Issue.2, Pp. 1229-1237.

[3] Durowoju, M.O., Oladosu, K.O., and Akintan, A.L. (2013); "*Fractal Analysis of the Platelets in Al-Si Eutectic Cast Alloy*", International Journal of Engineering Science

and Technology, Vol. 5, Issue 5, Pp.1111-1119.

[4] Hussein A. A., Haidar, A.H. and Nabil, L. A., (2013); "*Use of waste for the manufacture of Electric Power Transmission Wires*", International Journal of Engineering and Technology, Vol. 3, No. 9.

[5] Farahany, S., Ourdjini, A., Idris, M. H., Thai, L. T. (2011), "*Effect of bismuth on microstructure of unmodified and Sr-modified Al-7Si-0.4Mg alloys*", Transaction of Nonferrous Metal Society of China, Vol. 2, Pp. 1455 – 1464.

[6] Kósa, A., Gácsi, Z., and Dúl, J., (2012); "*Effects of Strontium on the Microstructure of Al-Si Casting Alloys*", Materials Science and Engineering, Vol. 37, Issue 2, Pp. 43–50.

[7] Kim, K, Seok, H, Kim, Y., Yoon, J., Lee, D.,Chung, C., and Han, D. (2006), "*Optimization of melt treatment for in-house recycling of Al-alloy scrap*", Journal of Ceramic Processing Research, Vol. 7, No. 3, Pp. 266 – 270.

[8] Lu, S.Z., and Hellawell, A. (1995) "*Fractal Analysis of Complex Microstructures in Materials*", Proceedings of MC95 International Metallographic Conference, ASM Pp. 115 - 119.

[9] Mandelbrot, B., B. (1983) "*The Fractal Geometry of Nature*", Freeman Publishers, London.

[10] Miller, W.S., Zhuang, L., Bottema, J., Wittebrood, A.J., De-Smet, P., Haszler, A. and Vieregge, A., (2000), "*Recent development in aluminium alloys for the automotive industry*", Materials Science and Engineering, A280, Pp. 37 – 49.

[11] Monroe, R. (2005), "*Porosity I casting*", American Foundry Society, Schaumburg, IL, USA, Vol. 4, Pp. 1- 28.

[12] Paraskevas, D., Kellens, K., Dewulf, W., Duflou, J. R., (2013), "*Closed and open loop recycling of aluminum: A Life Cycle Assessment perspective*", Proceedings of the 11th Global Conference on Sustainable Manufacturing.

[13] Stunová, B. B., (2012), "*Effect of strontium on the structure of non-binary casting alloys Al-Si*", Brno, Czech Republic, Vol. 5, Pp. 23 – 28.